Fault Location Using the Distributed Parameter Transmission Line Model

A. Gopalakrishnan, M. Kezunovic, S. M. McKenna, and D. M. Hamai

Abstract—Earlier work at Texas A&M University led to the development of transmission line fault location algorithms that were based on synchronized sampling of the voltage and current data from the two ends of the line. The line models used in the algorithms were based on lumped parameter models for electrically short lines, or lossless distributed parameter models for electrically long lines. In this paper, the lossless line model is modified to account for the series losses in the line. The line model equations are then solved in the time domain to accurately locate the fault. Testing of the modified algorithm is performed on a power system belonging to the Western Area Power Administration. Extensive EMTP based simulations are used to generate data that are supplied as inputs to the fault location algorithm. To make the testing as realistic as possible, detailed models of instrument transformers are used in the simulation of the various fault cases.

Index Terms—Electromagnetic transients, fault location, modeling, synchronized sampling.

I. Introduction

RESEARCHERS in power systems have investigated fault location techniques for a number of years. By accurately locating a fault, the amount of time spent by line repair crews in searching for the fault can be kept at a minimum. Thus service can be restored quickly.

Fault location techniques can be classified into those that use data from just one end of the transmission line and those that use data from both (all) ends of the line. Protective relays are basically single-ended fault locators. The accuracy of single-ended fault locators is affected by the assumptions that are made about the fault impedance, the source impedance and the in feed into the fault from the remote end source.

Two- or multi-ended fault location techniques are therefore more accurate than single-ended methods. The unknown fault resistance can be eliminated from the line model equations to estimate the location of the fault.

Multi-terminal fault location algorithms differ in the method in which they handle the voltage and current data.

Most algorithms are based on the computation of the post-fault, fundamental frequency voltage and current phasor. The required phasors are computed by either filtering the transient data [1]–[5], or by numerical processing techniques, [6]–[8].

The second class of algorithms are based on traveling wave methods. Lee [9], proposed and tested a method that time-tags

the arrival of the first high-frequency pulse due to a fault, at each end of the line. From a knowledge of the surge impedance of the line, the length of the line and the difference between the time of arrival of the first pulse at each line end, the fault location can be determined. Magnago, [10] proposed the use of wavelets to decompose the sampled voltage and current data to determine the time of arrival of the high frequency fault pulse.

Algorithms that use raw samples of voltage and current data are proposed in [11]–[14]. These methods apply the voltage and current samples to a specific model of the line. The unknown distance to the fault is then solved for in the time-domain. Cory and Ibe [11] proposed a distributed parameter line model for the transmission line. The voltage and current data from one end of the line is applied to this model and a profile of the voltage and current is built along the line. The method of characteristics is used to solve for the voltage profile. Criteria functions are computed from the voltage profiles to determine the fault position. Although the series resistance is used in the line model, the sampling frequency that is used is around 300 kHz, which does not make it suitable for field implementation.

In this paper, we present an extension to the fault location methods reported in [12] and [13]. The series line resistance, that was previously ignored, is modeled. Unlike the method, proposed by Ibe and Cory [11], data is acquired from both ends of the transmission line synchronously. The voltage and current profile is built as before and the fault position is computed from the profiles alone. The sampling frequency requirements are also quite modest, and in the range of 20 kHz. While this is still outside the capability of conventional monitoring equipment, it can be achieved by using special data acquisition hardware. The proposed algorithm is first tested using a model of a simple, 200 mile long three-phase transmission line and then a model of a complex power system belonging to the Western Area Power Administration (the Appendix). Simulations were carried out using the EMTP, with instrument transformers as part of the simulations.

II. Fault Location Algorithm

In this section, the fault location algorithm is described. Usually, the length of the transmission line determines the model of the line that will be used for either simulation or other applications like fault location. At Texas A&M, two kinds of algorithms were developed to handle these two cases.

- The short line algorithm for lines shorter than 50 miles: The line model used in this case is the simple lumped parameter element. A fully coupled, three-phase series R–L element represents the line. The details of the algorithm can be found in [12] and [13].
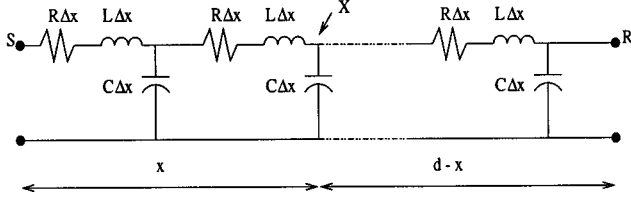
Fig. 1. Unfaulted long transmission line.

- The long line algorithm for lines longer than 150 miles: The shunt capacitance of the line begins to play an important part in the modeling of the transmission line, and therefore cannot be neglected. The parameters of the line have to be modeled as being distributed along the length of the line.

This leads to a model of the type shown in Fig. 1.

The development of the algorithm is carried out for the single phase line shown in the figure above. R, L and C are the series resistance, series inductance and the shunt capacitance of the line, measured in Ω, H and F per unit length respectively. They are assumed to be constant, but distributed uniformly along the line. The conductance of the line is neglected.

The voltage and current along the line are functions of the distance x from the end of the line and the time t. If we represent the voltage by $v(x, t)$ and the current by $i(x, t)$, these quantities can be related to the parameters of the line by the so-called *Telegrapher's Equations*:

$$\frac{\partial v}{\partial x} + L\frac{\partial i}{\partial t} = -Ri \tag{1}$$

$$C\frac{\partial v}{\partial t} + \frac{\partial i}{\partial x} = 0 \tag{2}$$

Partial differential (1) and (2) can be solved using the method of characteristics proposed by Collatz [15] explained below. To solve the equations, the required boundary conditions are the voltage and current samples from the two ends of the line over a period of around one clock cycle from the time of occurrence of the fault. Let these quantities be denoted by $v_S(0, t), i_S(0, t)$ for the sending end S of the line and by $v_R(0, t), i_R(0, t)$ for the receiving end R of the line (Fig. 1). The fault location problem is formulated as the process of finding the point on the line where the voltage computed using the sending end data and the voltage computed using the receiving end data are the same, or closest to each other, when compared to other points in the line.

A. Method of Characteristics

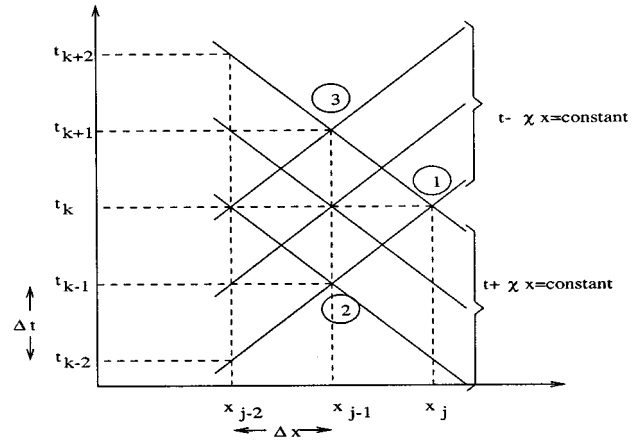We first make the following change of variables:

$$u = -Cv \qquad \chi = \sqrt{LC} \qquad \eta = RC \tag{3}$$

to get the modified *Telegrapher's Equations*:

$$\frac{\partial u}{\partial x} - \chi^2\frac{\partial i}{\partial t} = \eta i \tag{4}$$

$$\frac{\partial u}{\partial t} - \frac{\partial i}{\partial x} = 0 \tag{5}$$

The method of characteristics involves finding two curves, each of which is a function of the time t and position x. These curves are so chosen that the partial differential (4) and (5) reduce

Fig. 2. Characteristics in the x–t plane.

to simple differential equations. The two curves are called the *characteristics* of the solution.

For the system of (4) and (5), the characteristics are found to be $t \pm \chi x$ which are straight lines in the x–t plane. If we denote the length of the two characteristics by ρ and s, respectively, the differential equation relations between u and i can be written as

$$\frac{du}{ds} - \chi\frac{di}{ds} = \frac{\eta i}{\sqrt{1 + \chi^2}} \tag{6}$$

$$\frac{du}{d\rho} + \chi\frac{di}{d\rho} = \frac{-\eta i}{\sqrt{1 + \chi^2}} \tag{7}$$

The solution of (6) and (7) requires the discretization of the continuous time system. First, consider the Fig. 2 that shows the characteristics for a few points in the x–t plane. Let the x axis be discretized by the index j and the t axis by the index k.

We now want to develop an expression for the voltage and current at the point x_j at time t_k. Based on Fig. 2,

$$x_j - x_{j-1} = \Delta x \tag{8}$$

$$t_k - t_{k-1} = \Delta t \tag{9}$$

where

$$\Delta t = \chi \Delta x \tag{10}$$

Therefore,

$$\Delta s = \Delta \rho = \sqrt{\Delta x^2 + \Delta t^2} = \Delta x\sqrt{1 + \chi^2} \tag{11}$$

This allows us to integrate (6) and (7) using the trapezoidal rule, which after substituting for the voltage and current, yields the following explicit expressions:

$$v_{j,k} = \frac{1}{2}\left[v_{j-1,k-1} + v_{j-1,k+1}\right] + \frac{Z_c}{2}\left[i_{j-1,k-1} - i_{j-1,k+1}\right]$$
$$+ \frac{R\Delta x}{4}\left[i_{j-1,k-1} + i_{j-1,k+1}\right] - \frac{R\Delta x}{2}i_{j,k} \tag{12}$$

$$i_{j,k} = \frac{1}{2Z_c}\left[v_{j-1,k-1} - v_{j-1,k+1}\right] + \frac{1}{2}\left[i_{j-1,k-1} + k_{j-1,k+1}\right]$$
$$+ \frac{R\Delta x}{4Z_c}\left[i_{j-1,k+1} - i_{j-1,k-1}\right] \tag{13}$$

where $Z_c = \sqrt{L/C}$ is the surge impedance of the transmission line. From (12) and (13), we see that the voltage and current at
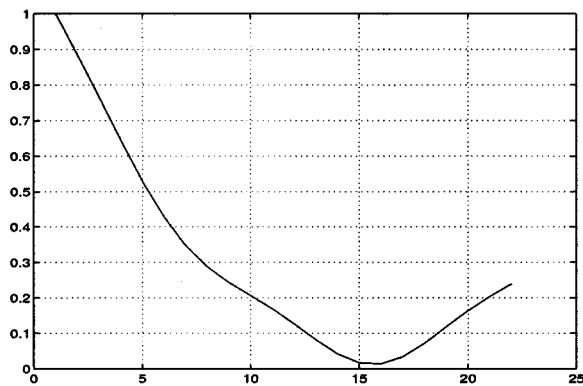
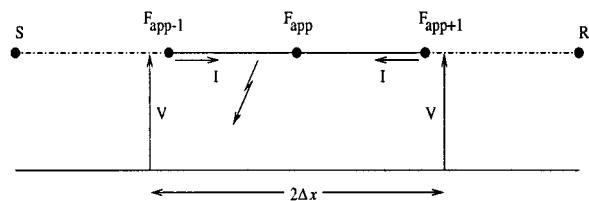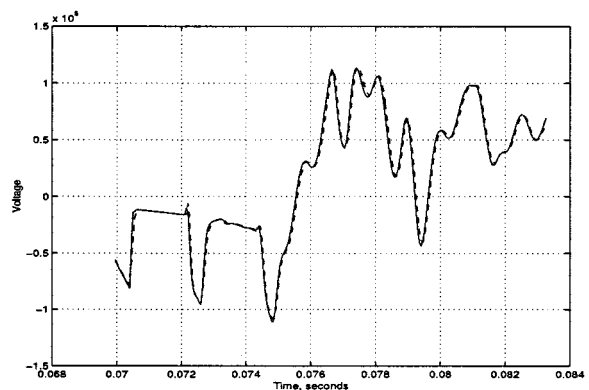Fig. 3. Location of approximate fault point.

Fig. 4. Refining the fault location.

Fig. 5. Reconstruction of Phase A voltage at point P. The solid line is the EMTP output, while the dashed line is the voltage as computed by the algorithm. Reconstruction begins when the fault is detected at the end S of the line.

any point x_j in the line, at time t_k, is a function of the voltage and current at the previous point in the line, x_{j-1}, at two different times, namely t_{k-1} and t_{k+1}. Thus, starting from the ends of the line, we can successively apply (12) and (13) to compute the voltage and current profile.

B. Steps in Fault Location

We now present the steps involved in the location of the fault using the method of characteristics.

- *Modal Decomposition*: The phase impedance and admittance matrices are used to determine the current transformation matrix T_i and the voltage transformation matrix T_v. The samples of phase voltage and current are transformed into ground mode and aerial mode values. We now have three decoupled single phase transmission lines.
- *Discretization of the Transmission Line*: Based on the sampling frequency of the data acquisition, the transmission line (each mode) is discretized into a finite number of points. For a value of the surge velocity equal to the speed of light (3×108 m/s), and a sampling interval of 50 μs, the length of each discrete segment is given by (10) to be approximately 9.32 miles. The method is therefore highly dependent on the sampling frequency.
- *Locate the Approximate Fault Point*: For each discrete point determined above, compute the voltage due to the sending end voltage and current, namely $v_S(0, t)$ and $i_S(O, t)$. Repeat the procedure using the receiving end data, namely $v_R(0, t)$ and $i_R(0, t)$. Plot the square of the difference between the two voltages so computed. Typically, a plot of the type shown in Fig. 3 is obtained. The discrete point that shows the least error is picked as the approximate fault point.
- *Refining the Fault Location*: This step involves reconstruction of the voltage and current data at the two discrete points that are on either side of the approximate fault point that was determined in the previous step. The adjacent points are denoted by F_{app-1} and F_{app+1} in Fig. 4. The actual fault location is assumed to be in the segment of length $2\Delta x$ around the approximate fault point F_{app}.

Now, the short line algorithm is applied to the segment of length $2\Delta x$. It should be noted that before applying the refinement, the reconstructed voltage and current values must be transformed back to the phase domain.

III. RESULTS FROM TESTING THE ALGORITHM

This section presents some results from testing the algorithm developed in the previous section. Testing is carried out on two systems as described below. All simulations are done in EMTP [16].

A. Simple Transmission Line

Here, a 200 mile long transmission line is considered. Series compensation capacitors are included in the system model. A Phase A to ground fault is applied at the end of the transmission line, and the voltage and current, at a point 160 miles from the sending end (40.0 miles from the fault) are recorded using EMTP. The voltage and current profiles along the line are then computed using (12) and (13). Fig. 5 shows the reconstruction of the Phase A voltage at the point 160 miles distant from the sending end. Also shown is the actual voltage as determined by EMTP.

It is seen that the reconstruction is quite accurate, when compared to the EMTP output. Similarly accurate reconstructions were obtained for the other voltages and currents at the point P. When applied to the fault location problem, we can therefore expect that the reconstruction at the points F_{app-1} and F_{app+1} will be accurate enough for proper fault location.

B. Utility Transmission System

The testing of the algorithm was then carried out using data generated from the EMTP simulation of a real power system, belonging to Western Area Power Administration. The one line

TABLE I
MAXIMUM FAULT LOCATION ERROR (%) A–G FAULT

Actual Location	Error and Computed Location			
	PC	PN	SC	SN
40.0	0.355	0.708	1.498	1.604
	39.15	38.28	43.63	43.88
79.8	0.367	0.437	0.246	1.405
	80.68	80.86	80.40	83.21
160.0	1.076	1.128	1.084	1.196
	162.61	162.73	157.37	162.9
223.5	2.727	2.041	1.570	1.339
	230.11	228.45	227.30	226.75

TABLE II
MAXIMUM FAULT LOCATION ERROR (%) B–C FAULT

Actual Location	Error and Computed Location			
	PC	PN	SC	SN
40.0	1.650	1.833	0.402	0.098
	36.00	35.56	39.03	39.76
79.8	3.791	3.283	3.513	0.913
	70.61	71.84	71.28	77.59
160.0	3.013	1.526	2.880	0.848
	152.70	156.30	153.02	157.94
223.5	1.856	0.757	0.828	1.058
	228.00	225.34	221.49	220.93

diagram of the system is shown in the Appendix. The line of interest is the 525 kV line from the Mead to Westwing sub-station. The line is 242.4 miles long and is mutually coupled to the 345 kV Mead–Liberty line for 204.9 miles, starting from Mead. There is also a 16.73 mile section, that is mutually coupled to two 525 kV lines starting at Palo Verde and terminating at Westwing. The Mead–Westwing and Mead–Liberty lines are equipped with series compensation capacitors at each end. The capacitors are protected by Metal Oxide Varistors (MOV's). For a detailed description of the system, please see [13, Section III].

The voltage and current data are acquired from the Mead 525 and 345 kV buses, the Westwing 525 kV bus and the Liberty 345 kV bus, to give a total of 4 three phase voltages and 4 three phase currents. No data is available from the Palo Verde–Westwing double line.

On this system, extensive EMTP simulations were carried out, with the following variations in the simulation conditions:

- *Fault Locations*: Faults were introduced at 40.0, 79.8, 160.0, and 223.5 miles from Mead.
- *Fault Types*: Four types of faults were considered; *viz.* Phase A to Ground, Phase B to C, Phase B to C to Ground and Three Phase to Ground.
- *Fault Incidence Angle*: 0° and 90°.
- *Fault Impedance*: 3 Ω and 50 Ω.
- *Series Capacitors*: Capacitors In and Capacitors Bypassed.
- *Instrument Transformers*: Data collected from the primary of from the secondary of the instrument transformers. The instrument transformer models used in this study were developed earlier [17], [18].

This gives a total of $4 \times 4 \times 2 \times 2 \times 2 \times 2 = 256$ test cases.

C. Testing Results

Tables I and II show the results for Phase A to Ground faults, and Phase B to C faults. Each column in the tables correspond to the following four system conditions respectively:

- PC: Data from Primary, with Series Capacitors
- PN: Data from Primary, without Series Capacitors
- SC: Data from Secondary, with Series Capacitors
- SN: Data from Secondary, without Series Capacitors

The error % is shown in each cell of the table, and below it is the distance as computed by the fault location algorithm. The error % is the worst case error of four different fault scenarios

which are obtained for two fault impedances and two incidence angles. The error is calculated by the formula given below:

$$Error\ (\%) = \frac{|Actual\ loc. - Computed\ loc.|}{Line\ Length} \times 100\%\quad (14)$$

The sampling frequency is 20 kHz. All distances are measured in miles from Mead substation. The single line to ground fault shows a better accuracy than the multi-phase fault for most of the testing scenarios. The accuracy of the fault location when the data is measured at the primary of the instrument transformers (scenarios PC and PN) is a little better than when the data is measured at the secondary (scenarios SC and SN), for a number of cases. The largest error occurs for the Phase A to Ground Fault at 223.5 miles from Mead, with the series capacitors included in the simulation and with the data measured at the primary. Other than this, there is no clear pattern in the error percentages. The testing also showed that the maximum errors were not associated with one particular fault incidence angle or fault impedance. Errors for the Phase B to C fault are higher in general, than the errors for the single line to ground fault. When data is measured from the secondary of the instrument transformers, the error percentages are lower than the cases when data is measured from the primary. The largest error is 3.791% for a fault at 79.8 miles from Mead, with the series capacitors included and data taken from the primary. This corresponds to a error in the fault location of 9.19 miles. The lowest errors are seen for faults at 40.0 miles. At 79.8 and 160.0 miles from Mead, the errors increase, and then drop again at 223.5 miles. As in the case of the Phase A to Ground fault, there was no association between the maximum error and any particular incidence angle or fault impedance.

D. Factors Affecting the Fault Location Accuracy

One of the main factors affecting the fault location is the sampling frequency of the data. The sampling interval determines the length of each discrete segment of the long transmission line, as per Equation (10). In our algorithm however, the fault location does not stop with determining the approximate point. It is further refined by applying the short line algorithm on a segment of the line around the approximate fault point. Therefore, the sampling frequency does not play as important a role as it does for the authors in [11]. However, the sampling frequency must be high enough to ensure that the refinement of the fault location is carried out on a segment that is reasonably short. In our

case, this segment is around 16 miles, at a sampling frequency of 20 kHz.

The main factors affecting the accuracy of the fault location are:

- *Transposition Points in the Power System*: Looking at Fig. 6, transposition points are seen at 79.8, 160.0, 204.9 and 223.5 miles in the line. These points are sources of reflected traveling waves, which affect the terminal voltage and current data. Our algorithm however, considers the line to be made up of three homogeneous sections: Mead to Fault Point, Fault Point to end of Mutual Coupling (204.9 Miles) and from 204.9 Miles to Westwing. If the fault is outside the mutually coupled section, then the algorithm assumes that the line is made up of two homogeneous sections. The reflections from the transposition points affect the accuracy of the voltage and current reconstruction at the points adjacent to the approximate point, which in turn affects the accuracy of the fault location.
- *Mutual Coupling with the Palo Verde Lines*: There is one section 16.73 miles long, where the Mead–Westwing line is coupled with two 525 kV line from Palo Verde. This coupling is not considered by the algorithm and is another source of error.

Not modeling components like series capacitors and surge arresters in the fault location algorithm did not affect the accuracy of the algorithm. As can be seen from the results, there is no clear trend to indicate if the presence or absence of the series capacitors in the simulations, affected the errors in any way, since all voltage and current measurements were taken from the line side of the circuit breakers.

IV. CONCLUSION

A fault location algorithm based on the distributed parameter model of the transmission line has been presented. This method extends upon the work on the lossless line model shown in [12], [13]. It is different from the method of [11] in the sense that it uses data from both ends of the transmission line, and also uses a sampling frequency that is much smaller (20 kHz) compared to the 300 kHz sampling frequency used in [11]. The method of characteristics is used to solve the transmission line model.

The algorithm is tested on the data generated from a number of EMTP simulations on a power system belonging to the Western Area Power Administration. Mutual coupling is present between two of the transmission lines for 204.9 miles of the total 242.4 miles. The algorithm is capable of locating faults within or outside the mutually coupled section. All it needs is the voltage and current data from the various line terminals. Except for antialiasing filters, no additional filtering of data is necessary.

Testing was carried out for a number of fault scenarios. To make the testing realistic, transient models of instrument transformers were used in the simulations, [17], [18].

The results presented show the worst case error for each scenario. The largest error is seen to be 9.19 miles, for a Phase B

to C fault. The best performance is seen for a Phase B to C fault also—an error of 0.24 miles.

Future work on the algorithm will involve testing the algorithm with the presence of noise in the measurements. Since the sampling frequency required is 20 kHz, it is possible to implement the algorithm using data acquisition equipment built for this purpose. Such off-the-shelf components are available from manufacturers like National Instruments. Since data is obtained from both ends of the line, synchronization of the samples is required. This is possible using GPS receivers, which will generate the sampling clock for the data acquisition equipment.

APPENDIX
SAMPLE POWER SYSTEM
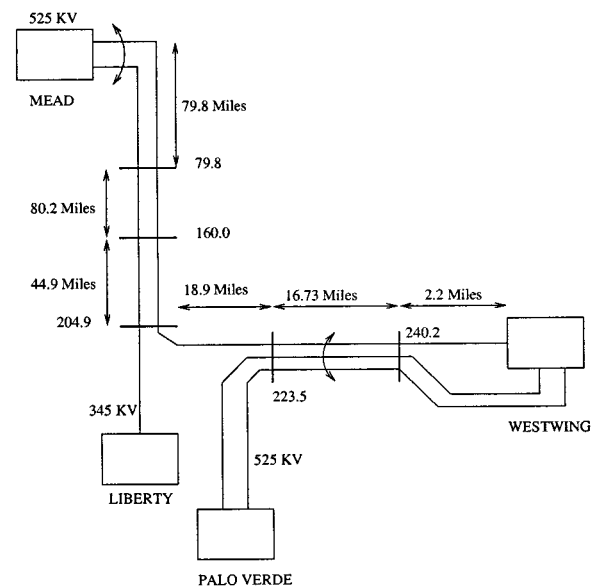
APPENDIX

A.1 Sample Power System

Fig. 6. One line diagram of the sample power system.

REFERENCES

[1] L. Erikson, M. M. Saha, and G. D. Rockefeller, "An accurate fault locator with compensation for apparent reactance in the fault resistance resulting from remote-end in feed," in *IEEE PES Summer Meeting*, Seattle, WA, July 15–20, 1984, Paper no. 84 SM-624-3.
[2] V. Cook, "Fundamental aspects of fault location algorithms used in distance protection," *IEE Proceedings*, pt. C, vol. 133, no. 6, Sept. 1986.
[3] M. S. Sachdev and R. Agarwal, "A technique for estimating transmission line fault locations from digital impedance relay measurements," *IEEE Trans. on Power Delivery*, vol. 3, no. 1, Jan. 1988.
[4] A. T. Johns, S. Jamali, and S. M. Haden, "New accurate transmission line fault location equipment," in *IEE Conference 302*, 1989.
[5] B. Jeyasurya and M. A. Rahman, "Accurate fault location of transmission lines using microprocessors," in *IEE Conference 302*, 1989.
[6] A. T. Johns and S. Jamali, "Accurate fault location technique for power transmission lines," *IEE Proceedings*, pt. C, vol. 137, no. 6, Nov. 1990.
[7] A. A. Girgis, D. G. Hart, and W. L. Peterson, "A new fault location technique for two- and three-terminal lines," *IEEE Trans. on Power Delivery*, vol. 7, no. 1, Jan. 1992.
[8] D. Novosel, D. G. Hart, and E. Udren, "Unsynchronized two terminal fault location estimation," *IEEE Trans. on Power Delivery*, vol. 11, pp. 130–138, Oct. 1996.

[9] H. Lee, "Development of an accurate traveling wave fault locator using global positioning satellites," in *Spring Meeting of the Canadian Electrical Association*, Montreal, Quebec, Mar. 1993.

[10] F. H. Magnago and A. Abur, "Accurate fault location using wavelets," *IEEE Trans. on Power Delivery*, vol. 13, no. 4, pp. 1475–1480, Dec. 1998.

[11] A. O. Ibe and B. J. Cory, "A traveling wave fault locator for two- and three-terminal networks," *IEEE Trans. on Power Systems*, vol. PWRD-1, no. 2, pp. 283–288, Apr. 1986.

[12] M. Kezunovic, J. Mrkic, and B. Perunicic, "An accurate fault location algorithm using synchronized sampling," *Electric Power Systems Research Journal*, vol. 29, no. 3, May 1994.

[13] S. M. McKenna, D. M. Hamai, M. Kezunovic, and A. Gopalakrishnan, "Transmission line modeling requirements for testing new fault location algorithms using digital simulators," in *Proceedings of the Second International Conference on Digital Power System Simulators*, Montreal, Quebec, May 1997.

[14] M. Kezunovic and B. Perunicic, "Automated transmission line fault analysis using synchronized sampling at two ends," *IEEE Trans. on Power Systems*, vol. 11, no. 1, pp. 441–447, Feb. 1996.

[15] L. Collatz, *The Numerical Treatment of Differential Equations*: Springer-Verlag, 1966.

[16] EPRI, "Electromagnetic transients program (EMTP)," in *Version 2, Revised Rule Book* Palo Alto, CA, Mar. 1989, vol. 1.

[17] M. Kezunovic, L. Kojovic, V. Skendzic, C. W. Fromen, D. R. Sevcik, and S. L. Nilsson, "Digital models of coupling capacitor voltage transformers for protective relay transient studies," *IEEE Trans. on Power Delivery*, vol. 7, no. 4, pp. 1927–1935, Oct. 1992.

[18] M. Kezunovic, L. Kojovic, A. Abur, C. W. Fromen, D. R. Sevcik, and F. Phillips, "Experimental evaluation of EMTP-based current transformer models for protective relay transient study," *IEEE Trans. on Power Delivery*, vol. 9, no. 1, pp. 405–413, Jan. 1994.

A. Gopalakrishnan received the B.E. (Hons.) degree in electrical and electronics engineering from BITS, Pilani, India in 1989, and the M.S. degree in electrical engineering from Texas A&M University in 1995. He is currently a Ph.D. candidate in electrical engineering at TAMU.

M. Kezunovic (S'77–M'80–SM'85–F'99) received his Dipl.Ing. degree from the University of Sarajevo, the M.S. and Ph.D. degrees from the University of Kansas, all in electrical engineering in 1974, 1977 and 1980 respectively. He has been with Texas A&M University since 1987 where he is a Professor and the Director of the Electric Power and Power Electronics Institute. His main research interests are digital simulators and simulation methods for relay testing as well as application of intelligent methods to power system monitoring, control and protection. Dr. Kezunovic is a Registered Professional Engineer in Texas and a Fellow of the IEEE.

S. M. McKenna earned his B.S. degree from the Colorado School of Mines in 1978. He joined the Western Area Power Administration in September 1980. He is currently in the Substation Control Branch where he is involved in control system design for advanced technology devices, protective relaying application and testing, and power system testing. He is a Registered Professional Engineer in Colorado.

D. M. Hamai received his B.S. and M.S. degrees in electrical engineering from the University of Colorado in 1986 and 1994 respectively. He has been employed with the Western Area Power Administration since 1986 and is currently in the System Control and Protection Section where he is involved with various EMTP studies, power system protection applications and major power equipment requirements. He is a Registered Professional Engineer in Colorado.